Electronic Supplementary Material (ESI) for Analyst.

Supplementary Data

Table of Contents

Table S1. List of proteins on the CoVariant protein microarray.

No.	Protein name	Catalog number	Provider
1	SARS2-ECD	40589-V08B1	Sino biological
2	D614G-ECD	40589-V08B6-100	Sino biological
3	B.1.1.7-ECD	40589-V08B5-100	Sino biological
4	B.1.351-ECD	40589-V08B9-100	Sino biological
5	P.1-ECD	40589-V08B8-100	Sino biological
6	B.1.617.2-ECD	40589-V08B16	Sino biological
7	B.1.617.3-ECD	40589-V08B17	Sino biological
8	B.1.529-ECD	GTX136780-pro	Genetex
9	BA.2.12.1-ECD	SPN-C522d	Acro Biosystems
10	BA.4-ECD	SPN-C5229	Acro Biosystems
11	BA.5-ECD	SPN-C522e	Acro Biosystems
12	SARS2-RBD	40592-V08B	Sino biological
13	B.1.1.7-RBD	40592-V08H82	Sino biological
14	B.1.351-RBD	40592-V08H85	Sino biological
15	P.1-RBD	40592-V08H86	Sino biological
16	B.1.617.2-RBD	40592-V08H90	Sino biological
17	B.1.617.3-RBD	40589-V08B17	Sino biological
18	B.1.1.529-RBD	40592-V08H121	Sino biological
19	BA.2.12.1-RBD	40592-V08H132	Sino biological
20	BA.4-RBD	40592-V08H130	Sino biological
21	BA.5-RBD	40592-V08H131	Sino biological
22	SARS2-N	40588-V08B	Sino biological
23	B.1.529-N	40588-V07E34	Sino biological
24	Cell membrane mix (HEK, THP1, CaCo2, and A549)	Membrane extract kit 89842	ThermoFisher
25	Cy3+Cy5 landmark	H-109-105-008 and H-109-165-148	Jackson Laboratory
26	BSA	A7906	Sigma
27	Protein A	P2165	Sigma

Figure S1. CoVariant Protein Array Layout.

A

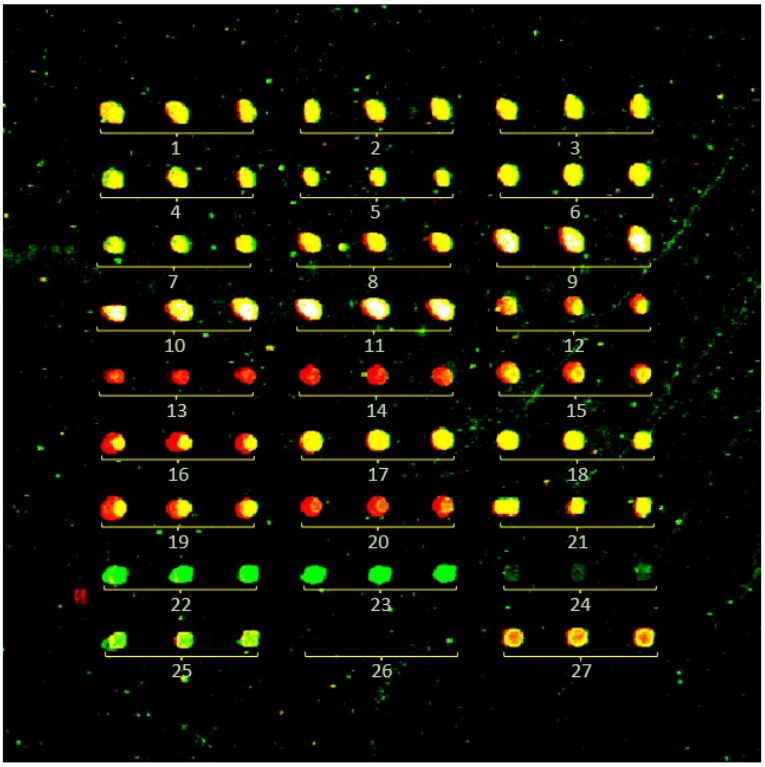

B

No.	Protein name
1	SARS2-ECD
2	D614G-ECD
3	B.1.1.7-ECD
4	B.1.351-ECD
5	P.1-ECD
6	B.1.617.2-ECD
7	B.1.617.3-ECD
8	B.1.529-ECD
9	BA.2.12.1-ECD
10	BA.4-ECD
11	BA.5-ECD
12	SARS2-RBD
13	B.1.1.7-RBD
14	B.1.351-RBD
15	P.1-RBD
16	B.1.617.2-RBD
17	B.1.617.3-RBD
18	B.1.1.529-RBD
19	BA.2.12.1-RBD
20	BA.4-RBD
21	BA.5-RBD
22	SARS2-N
23	B.1.529-N
24	Cell membrane mix (HEK, THP1, CaCo2, and A549)
25	Cy3+Cy5 landmark
26	BSA
27	Protein A

(A) Representative image of a single block on CoVariant Protein Array, stained with Cy3-labeled anti-human IgG+A+M antibodies and biotinylated human ACE2 and Cy5-conjugated streptavidin after plasma probing. (B) Protein name corresponding to protein triplets in block image.

Figure S2. Quality control of the CoVariant protein microarrays.

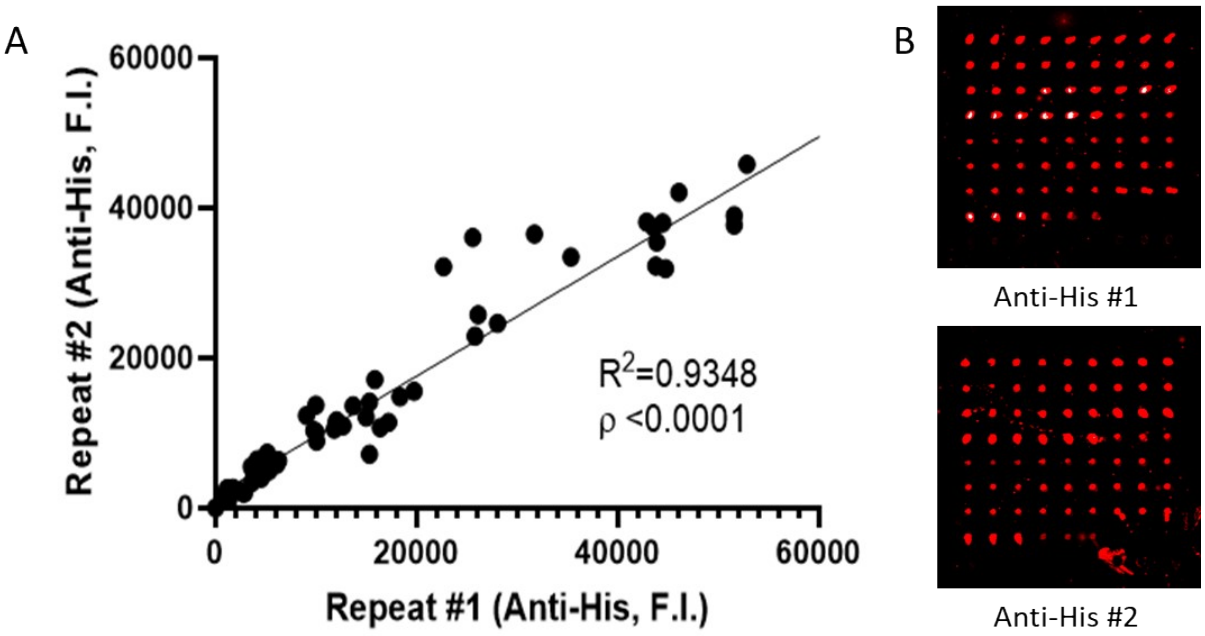

(A) The correlation of the two repeats of the anti-His staining. (B) The images of the anti-His staining with two individual repeats. Data were analyzed by the linear regression model.

Figure S3. Dual labeling of ACE2 and human antibodies on CoVariant protein arrays.

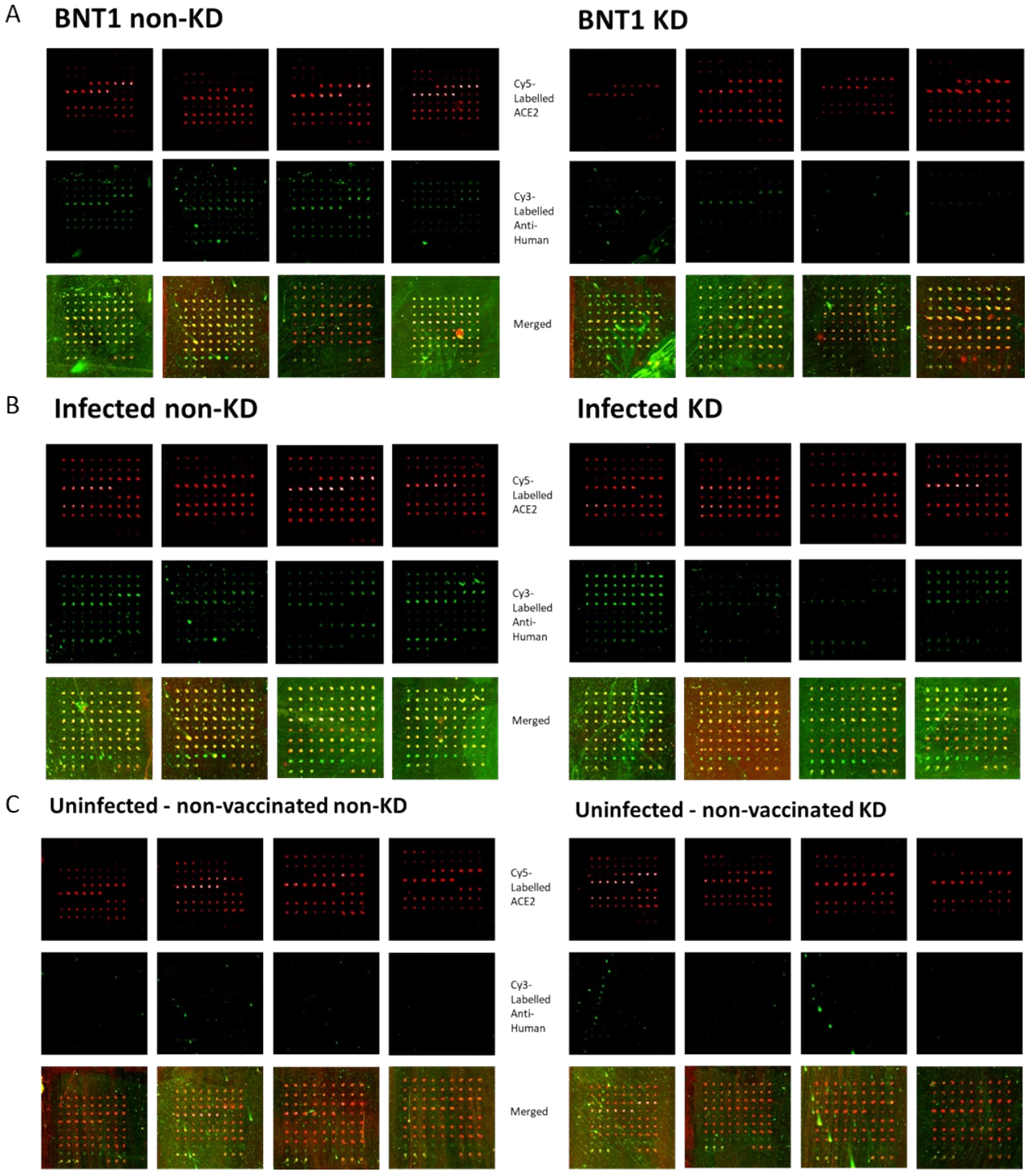

Each recombinant protein was printed in triplicate. Plasmas were incubated with pre-blocked CoVariant protein arrays for 1 hour, washed, and then incubated with Cy3-labeled anti-human and Cy5-labeled ACE2. After brief washing, the arrays were dried and scanned by the laser scanner. The representative images of Cy3 (green channel)

and Cy5 (red channel) labeling and their merged profiles for HC and KD groups for each category of (A) BNT1 (1-dose BNT162b2), (B) Infected and (C) Uninfected – unvaccinated (Pre-pandemic plasma).

Figure S4. Calibration of the CoVariant protein microarray by WHO reference panel 20/268.

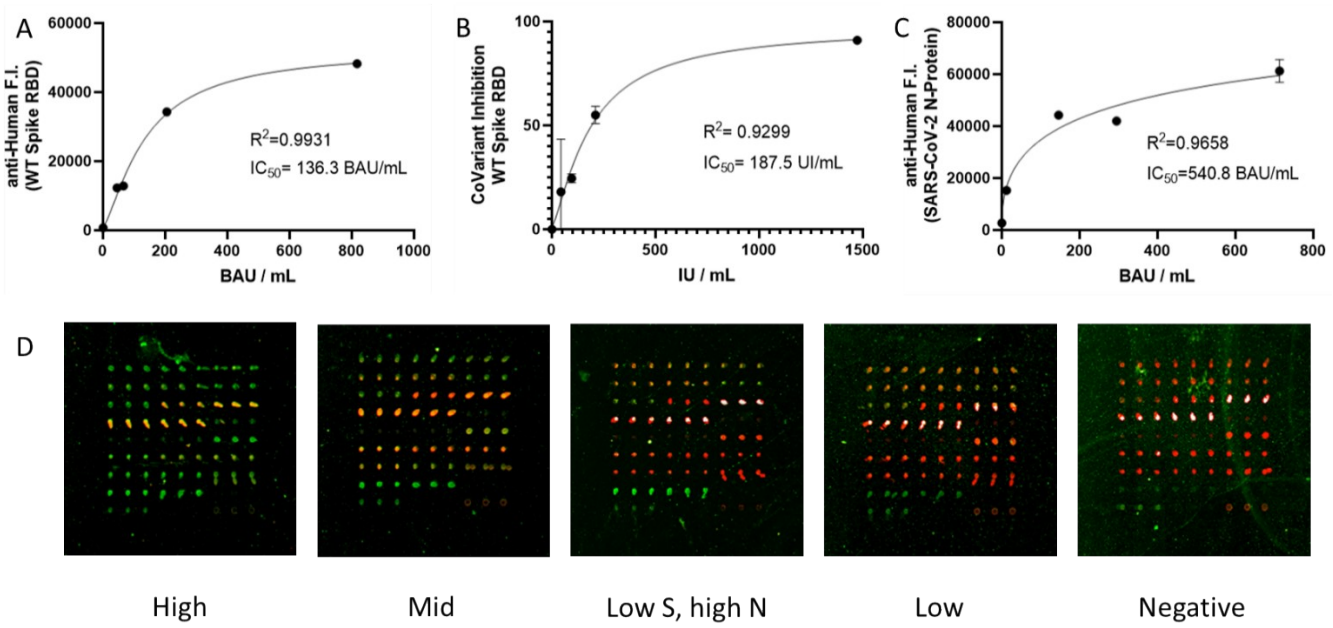

Anti-SARS-CoV-2 antibody titers were calibrated with WHO reference panel 20/268. (A) Anti-RBD IgG calibration curve. (B) Neutralization antibody calibration curve. (C) Anti-N IgG calibration curve. (D) Merged block images for binding and surrogate neutralization profiles for WHO reference samples.

Figure S5. Anti-N Protein levels of plasma for each category of participant subjects in the study.

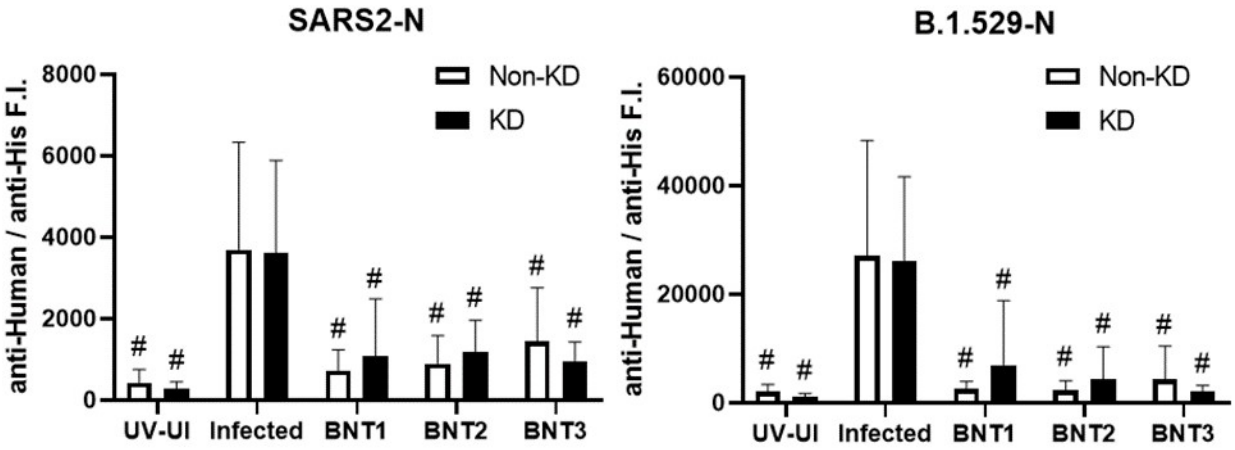

Anti-Nucleocapsid (N) protein antibody for HC and KD groups for each category of participants (A) Anti-N binding antibody levels against WT SARS-CoV-2. (B) Binding antibody levels against B.1.529 N-protein. Data were analyzed by Sidak's multiple comparisons among groups and subgroups, # $p < 0.05$ (all groups versus infected).

Figure S6. S-protein ECD binding antibody profiling for plasma by CoVariant Protein Microarray.

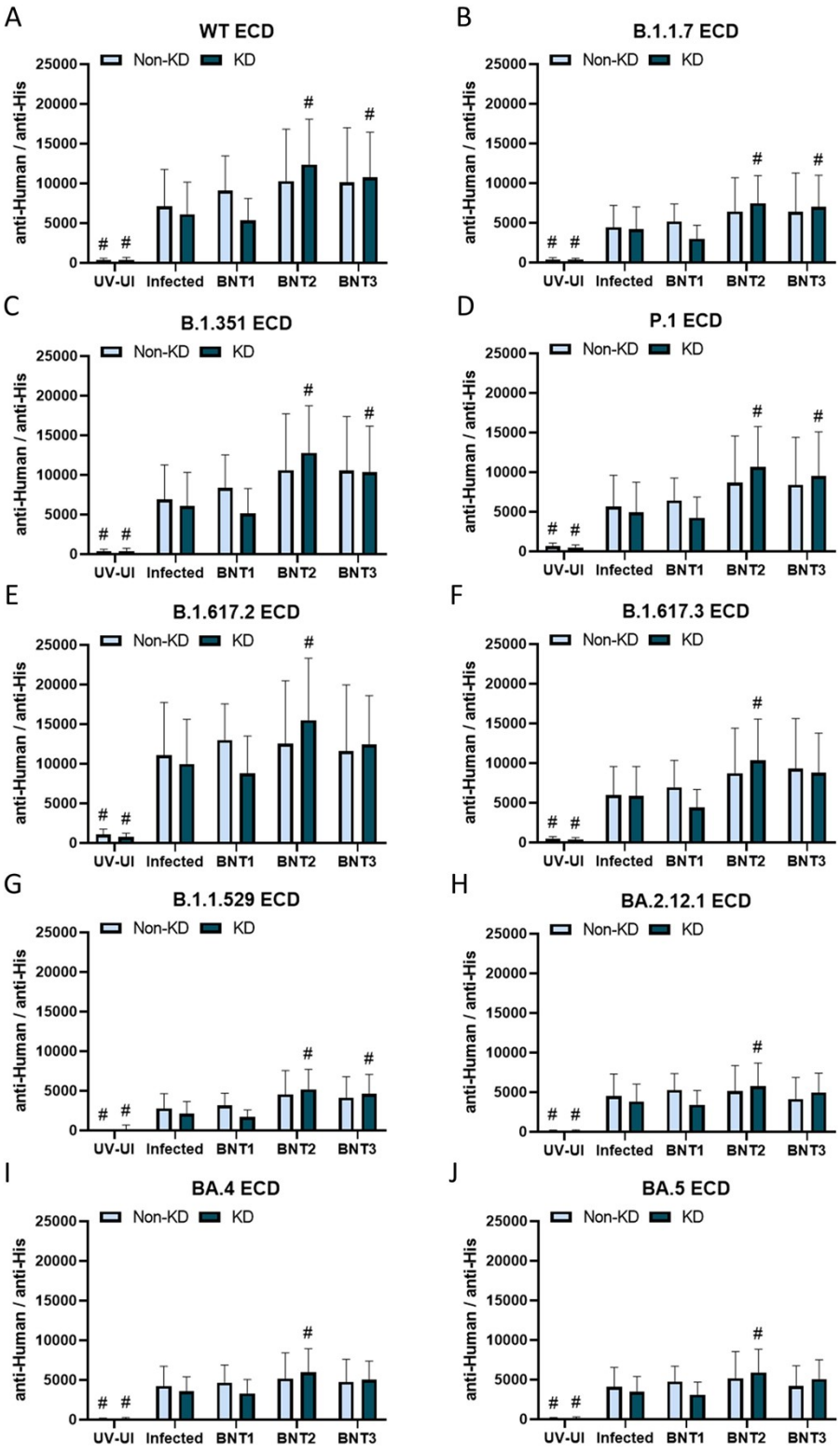

The binding antibody against S-protein ECD variants was measured based on the Cy3 anti-human signals divided by anti-His to normalize the protein amount immobilized on the CoVariant protein array. (A-J) The binding antibody of the plasma against the RBD of spike protein variants in unvaccinated-uninfected, infected, 1-dose BNT162b2, 2-dose BNT162b2, and 3-dose BNT162b2 subgroups for KD and HC. Data were analyzed by Sidak's multiple comparisons among groups and subgroups, # $p < 0.05$ (all groups versus infected).

Figure S7. S-protein ECD surrogate neutralizing profiling for plasma by CoVariant Protein Microarray.

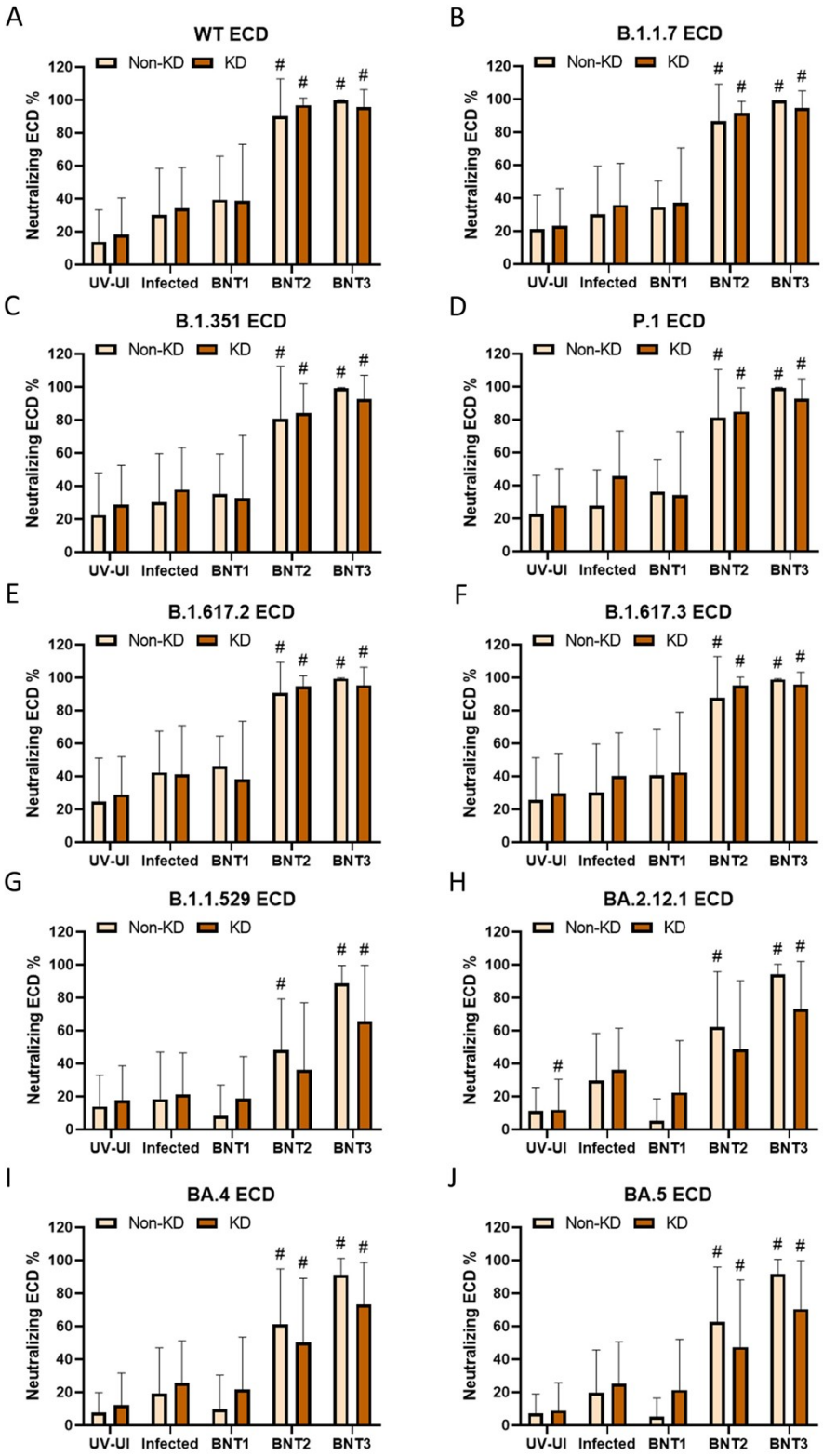

The surrogate neutralizing percentage against the variants of S-protein ECD was calculated based on the inhibition of ACE2 binding = 1 – (ACE2 with plasma/ACE2 without plasma) x 100%. (A-J) The surrogate neutralizing antibody of the plasma against the RBD of spike protein variants in unvaccinated-uninfected, infected, 1-dose BNT162b2, 2-dose BNT162b2, and 3-dose BNT162b2 subgroups for KD and HC. Data were analyzed by Sidak's multiple comparisons among groups and subgroups, # $p < 0.05$ (all groups versus infected).

Figure S8. Linear regression model for binding antibody vs. post-infection/vaccination time.

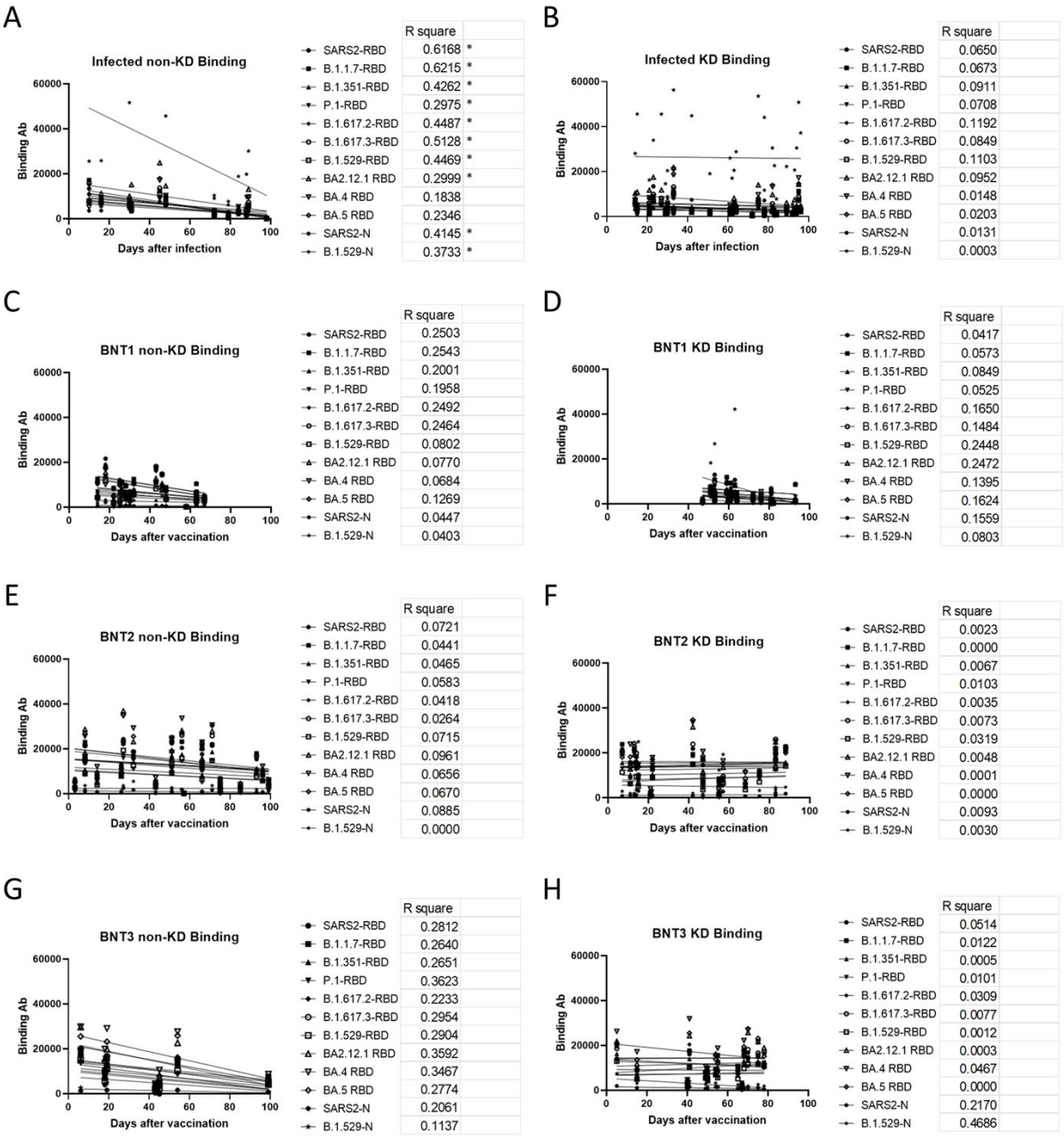

The binding antibody against S-protein RBD variants was correlated with post-infection/vaccination time. (A, B) Infected non-KD, infected KD. (C, D) BNT non-KD, BNT KD. (E, F) BNT2 non-KD, BNT2 KD. (G, H) BNT3 non-KD, BNT3 KD. Linear regression was used to calculate the R square and the significance. *$p < 0.05$.

Figure S9. Linear regression model for neutralizing antibody vs. post-infection/vaccination time.

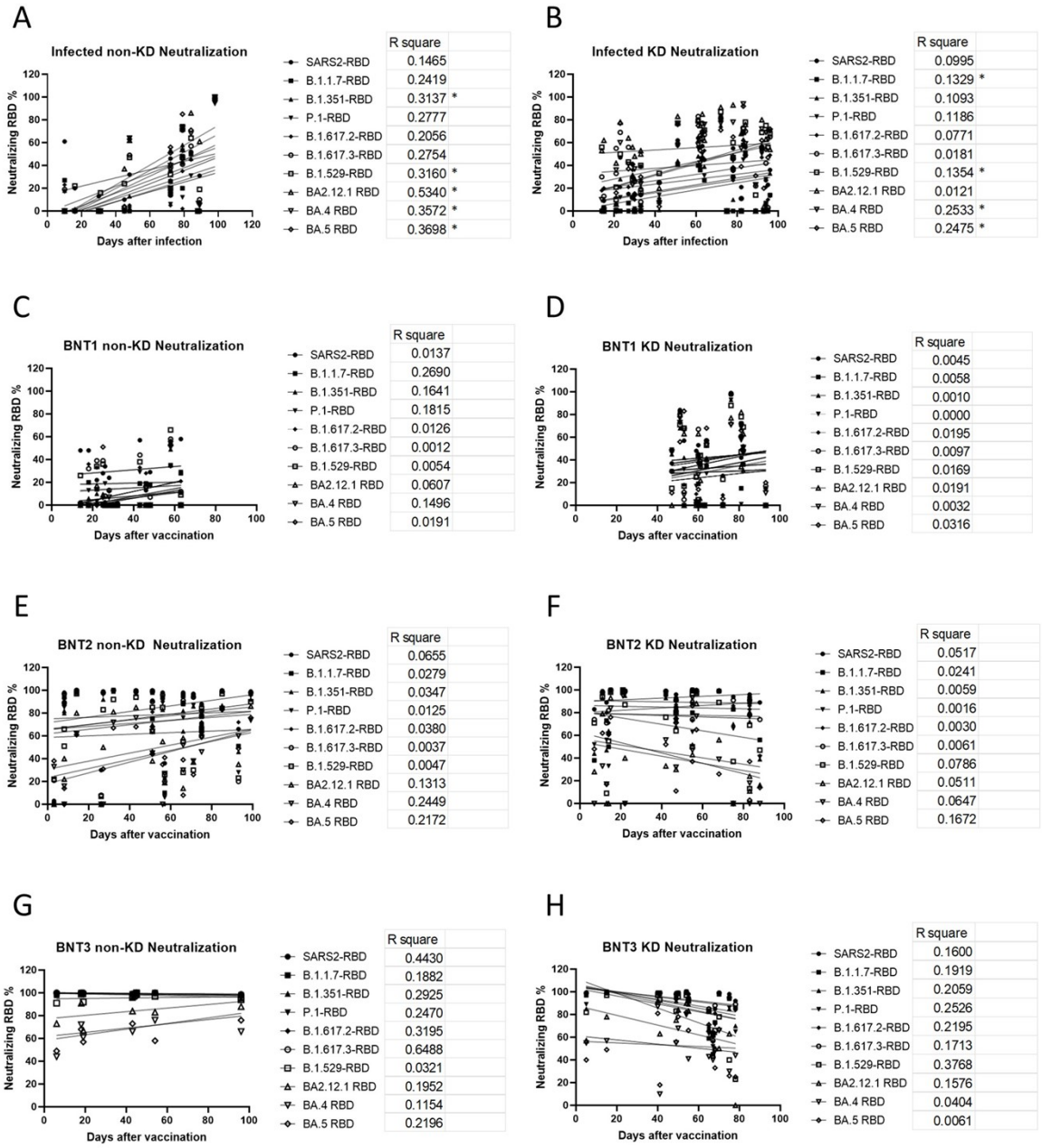

The neutralizing antibody against S-protein RBD variants was correlated with post-infection/vaccination time. (A, B) Infected non-KD, infected KD. (C, D) BNT non-KD, BNT KD. (E, F) BNT2 non-KD, BNT2 KD. (G, H) BNT3 non-KD, BNT3 KD. Linear regression was used to calculate the R square and the significance. *$p < 0.05$.

Figure S10. Linear regression model for binding antibody vs. post-IVIG infusion time and neutralizing antibody vs. post-IVIG infusion time.

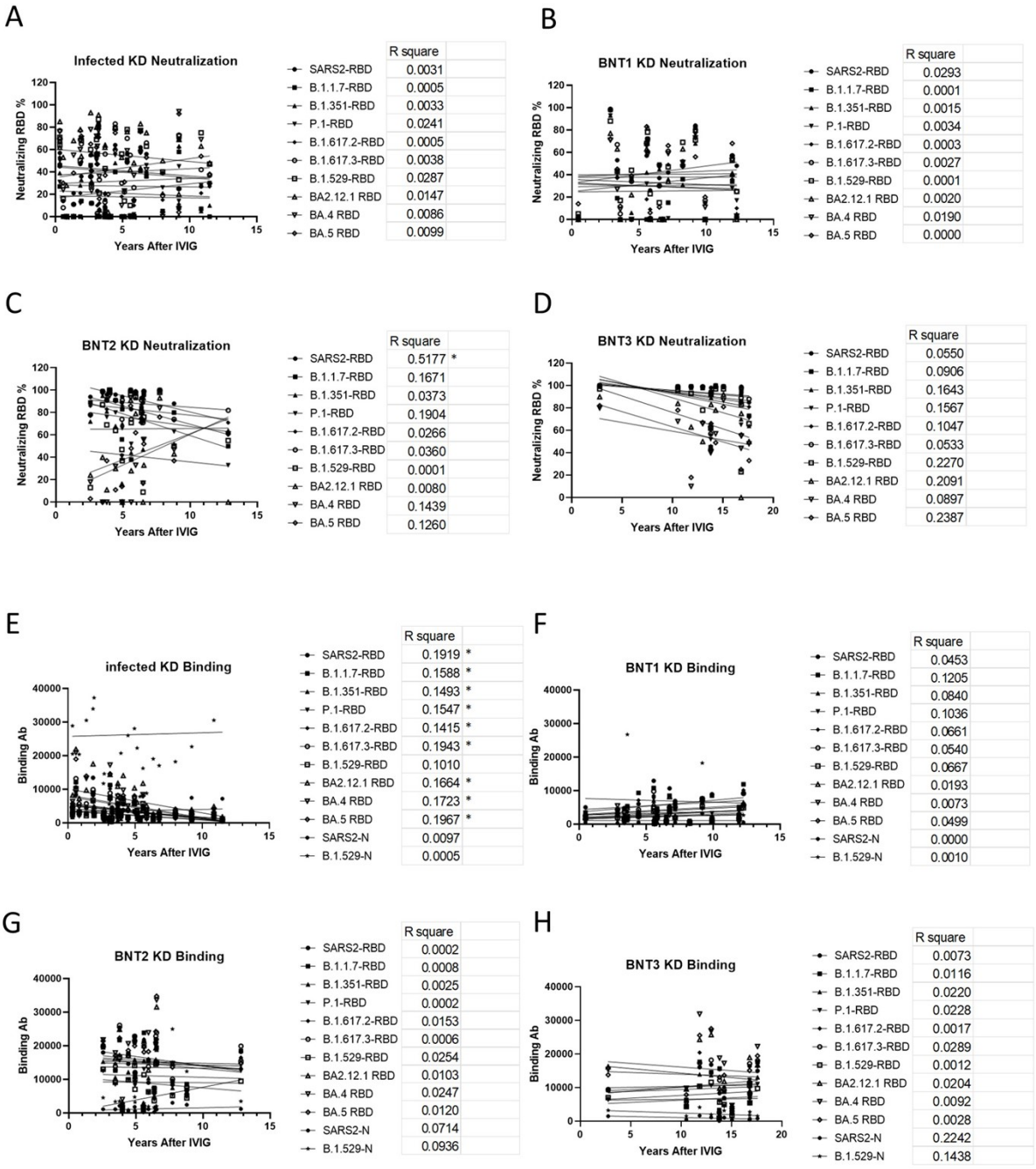

(A-D) The neutralizing antibody against S-protein RBD variants was correlated with post-IVIG infusion time in KD groups. (E-G) The binding antibody against S-protein RBD variants was correlated with post-IVIG infusion time in KD groups. Linear regression was used to calculate the R square and the significance. *$p < 0.05$.

Figure S11. Heatmap visualization of RBD binding antibodies and surrogate neutralizing capacities against S-protein variants.

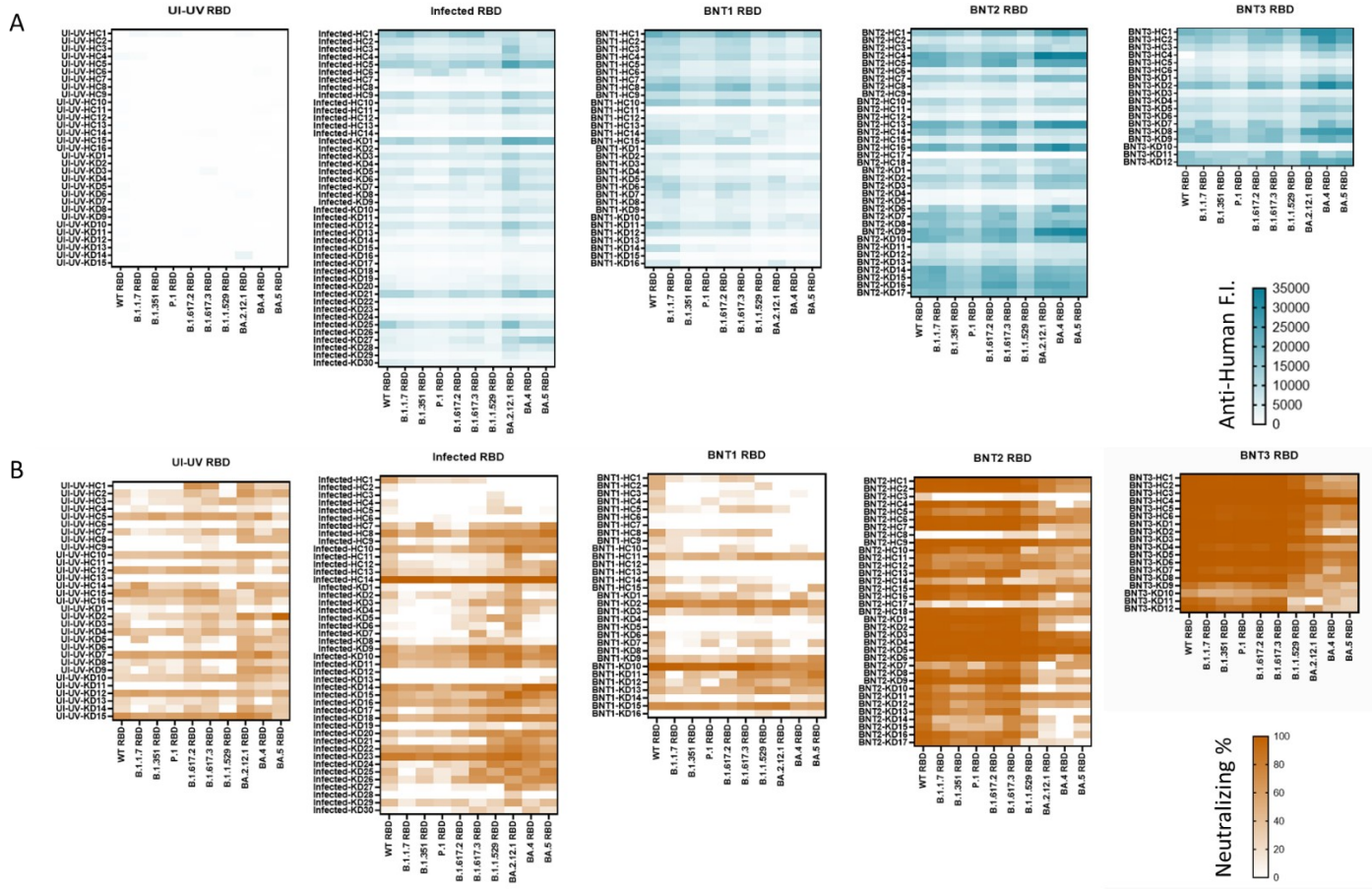

Plasmas from UI-UV, Infected, 1-dose BNT162b2, 2-dose BNT162b2, and 3-dose BNT162b2 vaccinated subjects were collected and analyzed for their (A) binding antibodies against RBDs by using CoVariant protein microarrays and (B) surrogate neutralizing antibody percentages against CoVariant RBDs. Each line stands for a subject in the corresponding category. The scales were labeled in the panel corner.

Figure S12. Heatmap visualization of ECD binding antibodies and surrogate neutralizing capacities against S-protein variants.

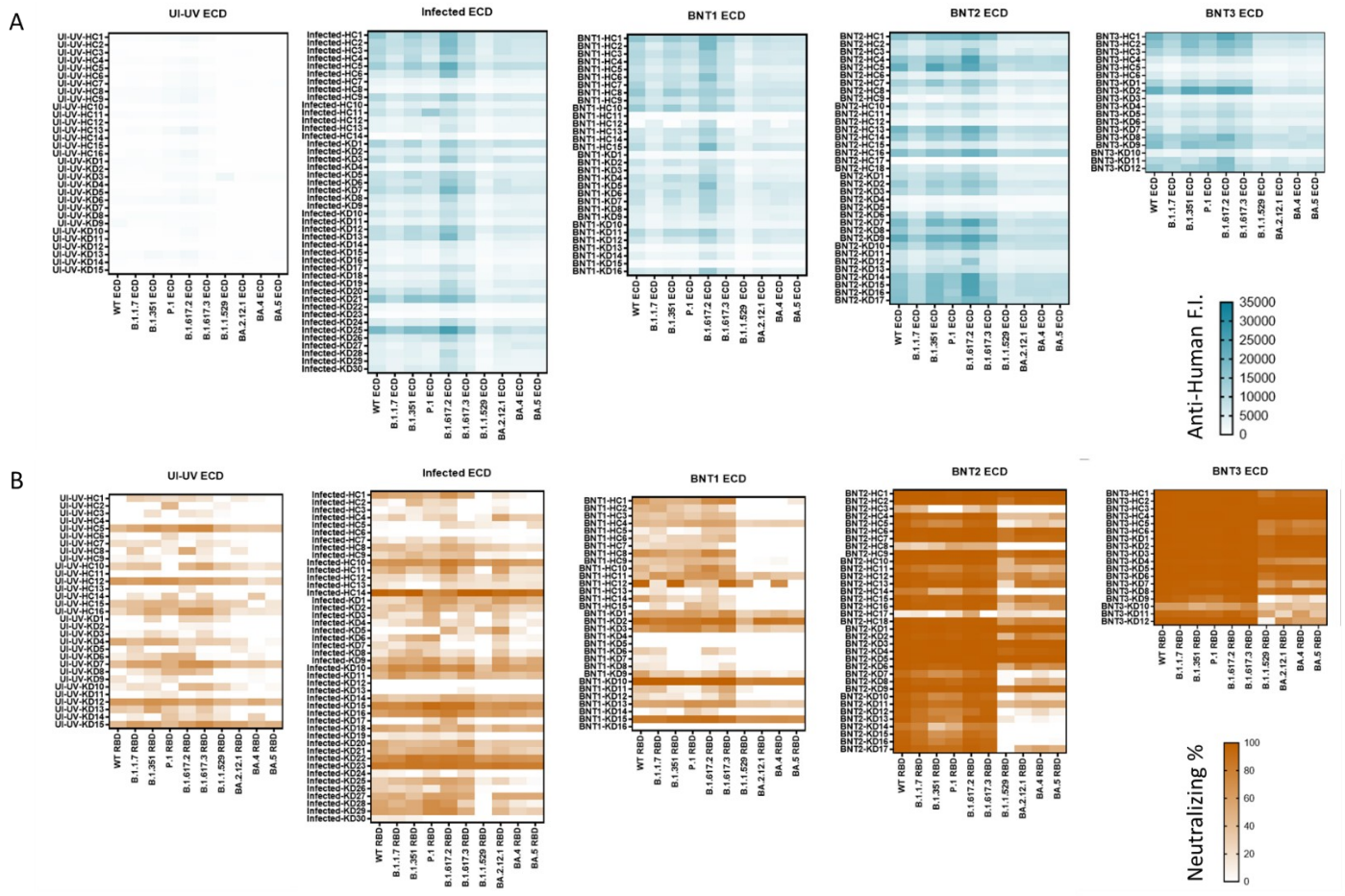

Plasmas from UI-UV, Infected, 1-dose BNT162b2, 2-dose BNT162b2, and 3-dose BNT162b2 vaccinated subjects were collected and analyzed for their (A) binding antibodies against RBDs by using CoVariant protein microarrays and (B) surrogate neutralizing antibody percentages against CoVariant RBDs. Each line stands for a subject in the corresponding category. The scales were labeled in the panel corner.